International Journal of Energy
ISSN: 2957-9473 | Vol. 9, No. 3, 2026

A Low Leakage Current Quasi-Z-Source Photovoltaic Inverter for New Energy Mountain Agricultural Machinery

Yunzhong Dai [1, 2], Hao Yu [3], Yi Wang [1], Yuhan Xie [1], Shiyi Liu [2], Kangle Guo [2], Teng Ma [1]

[1] Department of Mining and Architecture, Bijie Vocational and Technical College, Bijie, Guizhou, 551700, China
[2] Intelligent Manufacturing Institute, Yibin Vocational and Technical College, Yibin, Sichuan, 644003, China
[3] School of Mechanical Engineering, Sichuan University of Science & Engineering, Yibin, Sichuan, 643002, China

Abstract: The quasi-Z-source photovoltaic inverter offers advantages such as eliminating the need for dead-time, effectively suppressing high-frequency common-mode leakage current, eliminating the need for a bulky isolation transformer, and improving DC voltage utilization by inserting shoot-through vectors to boost the DC bus voltage. In contrast, traditional bridge-type grid-connected inverters suffer from drawbacks including the need for dead-time, large high-frequency common-mode leakage current, the requirement for a bulky isolation transformer, and low DC voltage utilization. To address these deficiencies, this paper first proposes a low-leakage-current quasi-Z-source photovoltaic inverter structure suitable for new energy agricultural machinery in mountainous areas. Next, the circuit topology and modulation strategy are presented, and the operating modes as well as the common-mode leakage current are analyzed. The research then shows that the proposed inverter not only eliminates the need for dead-time and effectively suppresses high-frequency common-mode leakage current, but also avoids the use of a bulky isolation transformer while effectively boosting the DC bus voltage and improving the DC voltage utilization of the grid-connected inverter. Finally, circuit simulation experiments verify the correctness of the inverter design and theoretical analysis.

Keywords: Photovoltaic Power Generation; Grid-connected; Inverter; Leakage Current; Quasi-Z-source; Mountain Agricultural Machinery; Dead-time-free.

1. Introduction

Agricultural machinery such as mountain intelligent tea harvesters and mountain intelligent prickly pear harvesters widely adopt new energy sources including photovoltaics and lithium batteries as power sources, and their performance has a significant impact on the operational efficiency and safety in mountainous and hilly areas. Compared with agricultural machinery using traditional fossil energy, new energy mountain intelligent agricultural machinery can not only effectively reduce the overall weight and volume of the machine, but also efficiently utilize solar energy, making it more suitable for use in mountainous and hilly regions. As a connection bridge between the DC power supply side and the load side of mountain new energy intelligent agricultural machinery, the inverter is required to stably provide pure sinusoidal AC power for the agricultural machinery's AI processor and AC drive motor. However, since intelligent agricultural machinery operates outdoors for extended periods, the parasitic capacitance of photovoltaic panels to ground in humid weather can easily induce leakage current, triggering protection mechanisms and threatening the safety of the entire machine. Relevant studies have shown that leakage current and common-mode characteristics are key issues for transformerless photovoltaic grid-connected inverters [1-4]. Therefore, leakage current suppression is one of the key issues that inverters must address. Conventional bridge-type grid-connected inverters require dead-time to be set for switches on the same bridge arm to avoid shoot-through, but the introduction of dead-time increases the harmonic content of the grid-connected current and reduces power quality. The existing Z-source/quasi-Z-source inverter topology, by adding a unique impedance network between the input power supply and the inverter bridge, breaks the operating mode of conventional bridge-type inverters and allows a shoot-through state [5-11] in which the upper and lower bridge arms conduct simultaneously. By reasonably inserting shoot-through vectors into the inverter bridge, the quasi-Z-source network can effectively boost the DC bus voltage. Compared with the two-stage topology combining a DC-DC boost converter and a conventional inverter, the quasi-Z-source bridge inverter can improve system efficiency, enhance reliability, and reduce costs [6-12]. However, transformerless photovoltaic inverters may suffer from high-frequency variations in common-mode voltage, resulting in significant common-mode leakage current, which makes it difficult to comply with leakage-current requirements [1-4]. To connect to the AC side, an isolation transformer is required, which increases the system volume and cost and reduces power density. To address this drawback, this paper first adopts the quasi-Z-source inverter topology and proposes corresponding modulation strategies and common-mode voltage suppression methods. Subsequently, its topological structure, modulation strategy, common-mode leakage current characteristics, and control methods will be analyzed.

2. Circuit Topology and Modulation Strategy

2.1. Circuit Topology

The low-leakage-current quasi-Z-source photovoltaic inverter proposed in this paper is shown in Figure 1, which includes a pre-stage quasi-Z-source circuit, power switches S_1-S_5, high-performance diodes D_1-D_3, a photovoltaic DC power source U_{dc}, and an AC-side symmetric filter circuit. The positive terminal of the photovoltaic DC power source

U_{dc} is connected to the pre-stage quasi-Z-source circuit, and the other terminal of the pre-stage quasi-Z-source circuit is connected to the collector of switch S_5. S_1 is connected in series with D_1, and D_2 is connected in series with S_2, with both branches connected in parallel to the emitter of S_5. The AC-side symmetric filter circuit and the pre-stage quasi-Z-source circuit are connected in parallel across the positive and negative terminals of U_{dc}. The pre-stage quasi-Z-source circuit includes filter inductors L_1 and L_2, filter capacitors C_1 and C_2, and diode D_3. The dotted terminal of L_1 is connected to the positive terminal of U_{dc}, and the undotted terminal of L_1 is connected to the anode of D_3. The cathode of D_3 is connected to the dotted terminal of L_2, and the undotted terminal of L_2 is connected to the collector of S_5. C_2 is connected in parallel between the undotted terminal of L_1 and the undotted terminal of L_2, and C_1 is connected in parallel between the anode of D_3 and the negative terminal of U_{dc}. This quasi-Z-source network can boost the DC bus voltage [6-8] in the shoot-through state and suppress input current ripple. The AC-side symmetric filter circuit includes the AC-side voltage u_g, filter inductors L_3 and L_4, and switches S_3 and S_4. The negative terminal of u_g is grounded, and the positive terminal is connected to L_3, with the other terminal of L_3 connected to the emitter of S_3. The negative terminal of u_g is also connected to L_4, and the other terminal of L_4 is connected to the emitter of S_4. S_3 and S_4 are connected in parallel, and the AC-side current is i_g. This symmetric filter circuit can effectively filter out high-frequency switching ripple, ensuring the sinusoidal quality of the grid-connected current.

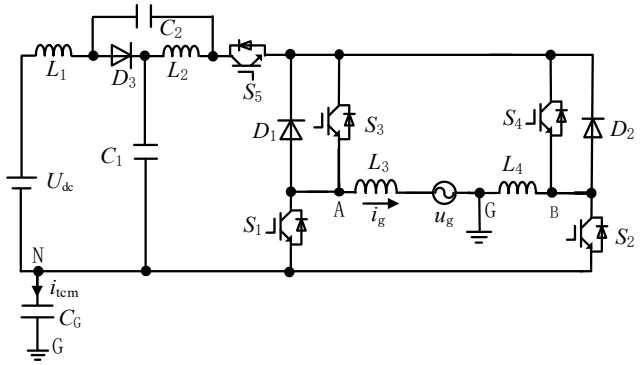

Figure 1. Schematic diagram of the circuit connection of a low-leakage-current quasi-Z-source photovoltaic inverter for new energy mountain agricultural machinery

2.2. Half-Cycle Modulation Strategy

The half-cycle modulation strategy of the inverter and the driving waveforms of switches S_1-S_5 are shown in Figure 2. In the figure, u_r is a unipolar triangular carrier wave, and u_c is the modulation wave. Switches S_1 and S_4 operate in the positive half-cycle; S_2 and S_3 operate in the negative half-cycle; S_5 switches at high frequency in the positive half-cycle and remains continuously on in the negative half-cycle. This modulation strategy can effectively reduce switching losses and improve inverter efficiency. By limiting the conduction interval of the switches to half of the power frequency cycle, the number of high-frequency switching actions is significantly reduced, thereby decreasing switching losses and thermal stress, while also simplifying the design of the driving circuit.

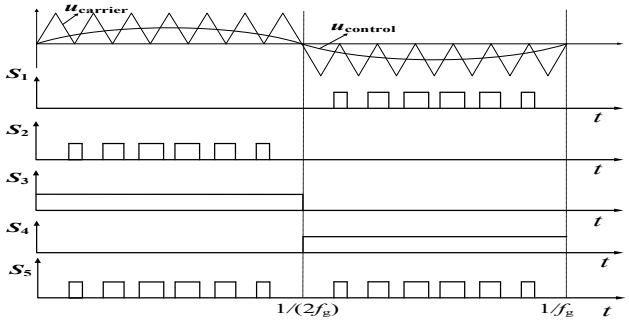

Figure 2. Half-cycle modulation and its driving waveforms

3. Operating Modes and Common-Mode Leakage Current Analysis

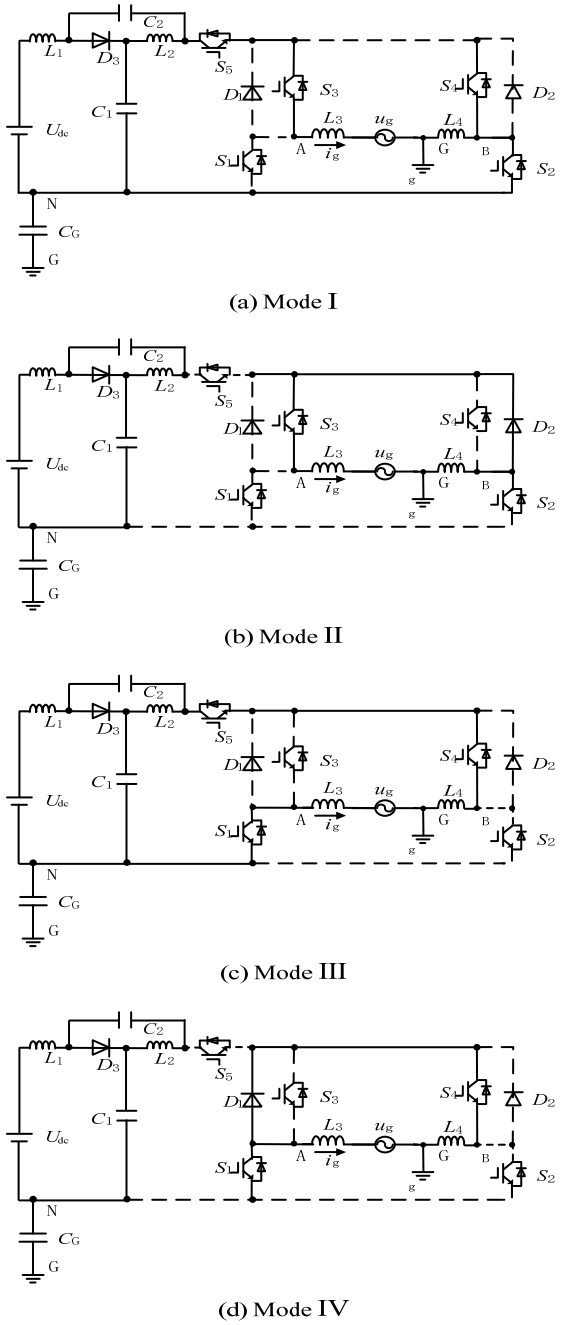

Figure 3. Equivalent circuit diagrams of each mode of a low-leakage-current quasi-Z-source photovoltaic inverter for new energy mountain agricultural machinery

The circuit connection of the proposed low-leakage-current quasi-Z-source photovoltaic inverter is shown in Figure 1,

and its half-cycle modulation strategy along with the driving waveforms of switches S_1-S_5 is shown in Figure 2. Based on the above circuit topology and modulation strategy, it is assumed that the AC-side current i_g is positive when flowing from point A to point G. According to the direction of i_g and the switching states of S_1-S_5, the system can operate in four operating modes, whose equivalent circuits are shown in Figures 3(a)~(d).

(1) Operating Mode I (i_g > 0, Shoot-Through Boost Mode)

When the proposed inverter circuit is in operation, operating mode I is as follows: power switches S_2, S_3, and S_5 are turned on, while power switches S_1 and S_4 are turned off, wherein the AC-side current i_g provided by the AC-side voltage u_g is greater than zero. Its equivalent circuit is shown in Figure 3(a). It can be seen from Figure 3(a) that D_1 and D_2 are reverse-biased and turned off, while D_3 is forward-biased and turned on, and U_{dc}, L_1, D_3, L_2, S_5, S_3, L_3, u_g, L_4, and S_2 form a forward charging closed loop, and i_g increases in the positive direction. Furthermore, according to Figure 3(a), we can obtain:

$$V_{\mathrm{G}} - V_{\mathrm{N}} = U_{\mathrm{dc}} - u_{\mathrm{g}} - I_{\mathrm{g}} \times j \times \omega_{\mathrm{SW}} \times L_3 \tag{1}$$

$$V_{\mathrm{G}} - V_{\mathrm{N}} = I_{\mathrm{g}} \times j \times \omega_{\mathrm{SW}} \times L_4 \tag{2}$$

In equations (1) and (2), V_G and V_N are the electric potentials at points G and N, respectively, $\omega_{SW} = 2\pi f_g$, and I_g is the RMS value of i_g. According to equations (1) and (2), the voltage across the distributed capacitor C_G, i.e., the common-mode voltage V_{NG}, in operating mode I of the low-leakage-current quasi-Z-source photovoltaic inverter for new energy mountain agricultural machinery is:

$$V_{\mathrm{NG}} = \frac{(u_{\mathrm{g}} - U_{\mathrm{dc}}) \times L_4}{L_3 + L_4} \tag{3}$$

(2) Operating Mode II (i_g > 0, Forward Freewheeling Mode)

Power switches S_3 and high-performance diode D_2 are turned on, while high-performance diode D_1, power switches S_1, S_2, S_4, and S_5 are turned off, wherein the AC-side current i_g provided by the AC-side voltage u_g is greater than zero. Its equivalent circuit is shown in Figure 3(b). L_3, u_g, L_4, D_2, and S_3 form a forward discharge freewheeling loop, and i_g decreases in the positive direction. This freewheeling path does not pass through the poor-performance body diode of the switch, reducing reverse recovery losses and improving inverter efficiency and reliability. From Figure 3(b), it can be seen that when S_5, S_3, and S_2 are the same type of switches, the voltage stresses across S_5, S_3, and S_2 are the same, i.e.:

$$V_{\mathrm{S_5}} = V_{\mathrm{S_2}} = V_{\mathrm{S_1}} \tag{4}$$

In equation (4), V_{S5}, V_{S3}, and V_{S2} are the voltages across switches S_5, S_3, and S_2, respectively. According to Figure 3(b) and Kirchhoff's voltage law:

$$\begin{aligned} V_{\mathrm{S_2}} + V_{\mathrm{S_5}} &= U_{\mathrm{dc}} \\ V_{\mathrm{S_1}} + V_{\mathrm{S_5}} &= U_{\mathrm{dc}} \end{aligned} \tag{5}$$

Combining equations (4) and (5) yields:

$$V_{\mathrm{S_1}} = V_{\mathrm{S_2}} = V_{\mathrm{S_5}} = \frac{U_{\mathrm{dc}}}{2} \tag{6}$$

Furthermore, according to Figure 3(b) and Kirchhoff's voltage law:

$$V_{\mathrm{G}} - V_{\mathrm{N}} = V_{\mathrm{S_1}} - u_{\mathrm{g}} - I_{\mathrm{g}} \times j \times \omega_{\mathrm{SW}} \times L_3 \tag{7}$$

$$V_{\mathrm{G}} - V_{\mathrm{N}} = V_{\mathrm{S_2}} + I_{\mathrm{g}} \times j \times \omega_{\mathrm{SW}} \times L_4 \tag{8}$$

According to equations (6), (7), and (8), the common-mode voltage V_{NG} in operating mode II of the low-leakage-current quasi-Z-source photovoltaic inverter for new energy mountain agricultural machinery is:

$$V_{\mathrm{NG}} = \frac{u_{\mathrm{g}} \times L_4}{L_3 + L_4} - \frac{U_{\mathrm{dc}}}{2} \tag{9}$$

(3) Operating Mode III (i_g < 0, Reverse Shoot-Through Boost Mode)

Power switches S_1, S_4, and S_5 are turned on, while high-performance diodes D_1 and D_2, and power switches S_2 and S_3 are turned off, wherein the AC-side current i_g provided by the AC-side voltage u_g is less than zero. Its equivalent circuit is shown in Figure 3(c). D_1 and D_2 are reverse-biased and turned off. U_{dc}, L_1, D_3, L_2, S_5, S_4, u_g, L_3, and S_1 form a reverse charging closed loop, and i_g increases in the negative direction. Furthermore, according to Figure 3(c) and Kirchhoff's voltage law:

$$V_{\mathrm{G}} - V_{\mathrm{N}} = U_{\mathrm{dc}} - i_{\mathrm{g}} \times j \times \omega_{\mathrm{SW}} \times L_4 \tag{10}$$

$$V_{\mathrm{G}} - V_{\mathrm{N}} = -u_{\mathrm{g}} + i_{\mathrm{g}} \times j \times \omega_{\mathrm{SW}} \times L_3 \tag{11}$$

According to equations (10) and (11), the common-mode voltage V_{NG} in operating mode III of the low-leakage-current quasi-Z-source photovoltaic inverter for new energy mountain agricultural machinery is:

$$V_{\mathrm{NG}} = \frac{u_{\mathrm{g}} \times L_4}{L_3 + L_4} - \frac{U_{\mathrm{dc}} \times L_3}{L_3 + L_4} \tag{12}$$

(4) Operating Mode IV (i_g < 0, Reverse Freewheeling Mode)

Power switch S_4 and high-performance diode D_1 are turned on, while power switches S_1, S_2, S_3, and S_5 are turned off, wherein the AC-side current i_g provided by the AC-side voltage u_g is less than zero. Its equivalent circuit is shown in Figure 3(d). S_4, D_1, L_3, u_g, and L_4 form a reverse discharge freewheeling loop. i_g decreases in the negative direction. This freewheeling path does not pass through the poor-performance body diode of the switch, reducing reverse recovery losses and improving inverter efficiency and reliability. Similar to the analysis of Mode II, the common-mode voltage of Mode IV can be obtained as:

$$V_{\mathrm{G}} - V_{\mathrm{N}} = \frac{U_{\mathrm{dc}}}{2} - u_{\mathrm{g}} - i_{\mathrm{g}} \times j \times \omega_{\mathrm{SW}} \times L_3 \tag{13}$$

$$V_{\mathrm{G}} - V_{\mathrm{N}} = \frac{U_{\mathrm{dc}}}{2} + i_{\mathrm{g}} \times j \times \omega_{\mathrm{SW}} \times L_4 \tag{14}$$

According to equations (13) and (14), the common-mode voltage V_{NG} in operating mode IV of the low-leakage-current quasi-Z-source photovoltaic inverter for new energy

mountain agricultural machinery is:

$$V_{\mathrm{NG}} = \frac{u_{\mathrm{g}} \times L_4}{L_3 + L_4} - \frac{U_{\mathrm{dc}}}{2} \tag{15}$$

Based on the above analysis, the switching states and V_{NG} of the low-leakage-current quasi-Z-source photovoltaic inverter for new energy mountain agricultural machinery are shown in Table 1:

Table 1. Operating Modes and Common-Mode Voltage

Half-Cycle	Mode	Common-Mode Voltage (VNG)
Positive Half-Cycle	I	$V_{\mathrm{NG}} = \frac{(u_{\mathrm{g}} - U_{\mathrm{dc}}) \times L_4}{L_3 + L_4}$
	II	$V_{\mathrm{NG}} = \frac{u_{\mathrm{g}} \times L_4}{L_3 + L_4} - \frac{U_{\mathrm{dc}}}{2}$
Negative Half-Cycle	III	$V_{\mathrm{NG}} = \frac{u_{\mathrm{g}} \times L_4}{L_3 + L_4} - \frac{U_{\mathrm{dc}} \times L_3}{L_3 + L_4}$
	IV	$V_{\mathrm{NG}} = \frac{u_{\mathrm{g}} \times L_4}{L_3 + L_4} - \frac{U_{\mathrm{dc}}}{2}$

From Table 1, it can be seen that when $L_3 = L_4$, the common-mode voltages V_{NG} of Modes I, II, III, and IV are the same, expressed as:

$$V_{\mathrm{NG}} = \frac{u_{\mathrm{g}} - U_{\mathrm{dc}}}{2} \tag{16}$$

4. Simulation Verification and Analysis

To verify the correctness of the proposed low-leakage-current quasi-Z-source photovoltaic inverter circuit topology and its common-mode leakage current analysis for new energy mountain agricultural machinery, a direct current control strategy is adopted for simulation verification. The system control block diagram is shown in Figure 4.

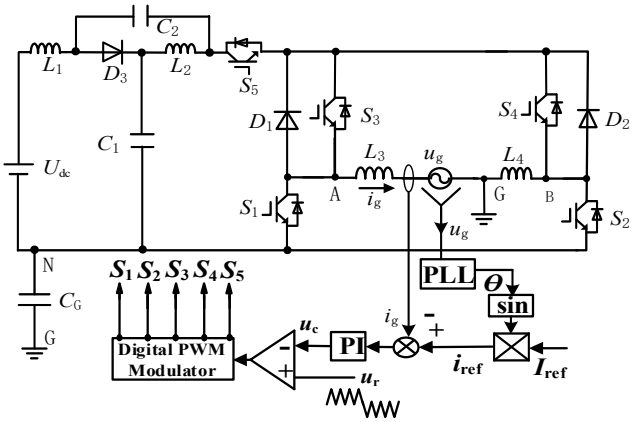

Figure 4. System circuit diagram composed of the low-leakage-current quasi-Z-source photovoltaic inverter for new energy mountain agricultural machinery

The phase-locked loop circuit obtains the phase angle *?* of the grid voltage u_g, and the DSP program looks up the corresponding sine table data sin*?*. The grid-connected current reference signal is then $i_{\mathrm{ref}} = I_{\mathrm{ref}}$? sin*?*. The deviation between i_g and i_{ref} is compared, and the modulation signal u_c is obtained through a PI regulator, thereby achieving the same phase between u_g and i_g. The circuit simulation parameters are shown in Table 2.

Table 2. Circuit Simulation Parameters

parameter	Value	Parameter	Value
U_{dc}	400V	C_{G}	75nF
U_m	220V	L_3=L_4	1.2mH
L_1=L_2	100uH	f_g	50Hz
f_{s}	10kHz	I_{ref}	20A
C_1=C_2	4000uF		

From Figure 5, it can be seen that using the above circuit simulation parameters, the waveforms of u_g and i_g are obtained. As shown in Figure 5, u_g and i_g maintain the same phase, indicating that the proposed low-leakage-current quasi-Z-source photovoltaic inverter for new energy mountain agricultural machinery has a high power factor.

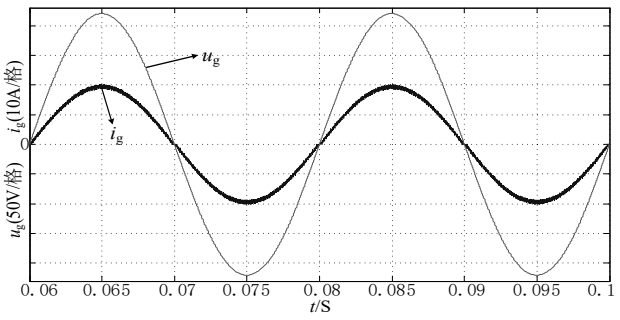

Figure 5. Simulation waveforms of i_g and u_g

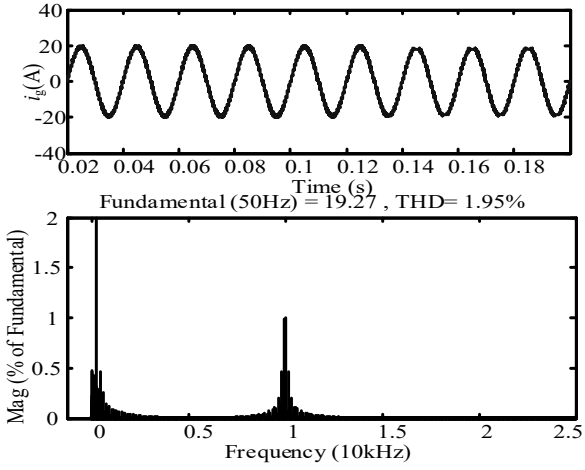

Figure 6. i_g and its FFT analysis diagram

Regarding i_g and its FFT analysis waveform, as shown in

Figure 6, i_g is a sinusoidal waveform with low distortion, and the total harmonic distortion (THD) is 1.95%. Since there is no need to set dead-time in the circuit simulation of the low-leakage-current quasi-Z-source photovoltaic inverter for new energy mountain agricultural machinery, the figure shows that the harmonics are mainly concentrated around the switching frequency of 5 kHz, with low-frequency harmonic components being relatively small. Therefore, the proposed low-leakage-current quasi-Z-source photovoltaic inverter for new energy mountain agricultural machinery has high grid-connected power quality.

Regarding the waveform of the effective common-mode voltage V_{NG}, as shown in Figure 7, the common-mode voltage V_{NG} contains only power frequency and DC components, with no high-frequency components, verifying the correctness of the common-mode voltage analysis for the low-leakage-current quasi-Z-source photovoltaic inverter for new energy mountain agricultural machinery.

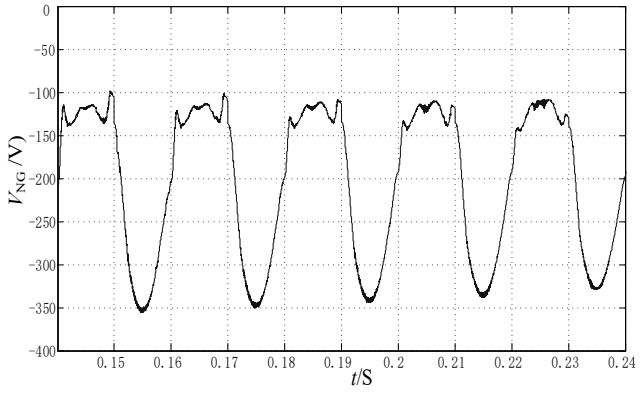

Figure 7. Simulation waveform of common-mode voltage V_{NG}

Regarding the common-mode leakage current i_{tcm} waveform, as shown in Figure 8, the peak value of the low-leakage-current quasi-Z-source photovoltaic grid-connected inverter provided in this paper within one power frequency cycle is approximately 100 mA, which is consistent with the leakage-current suppression requirement discussed in related photovoltaic grid-connected inverter studies [1-4]. Thus, the correctness of the circuit topology design and common-mode leakage current analysis of the low-leakage-current quasi-Z-source photovoltaic inverter for new energy mountain agricultural machinery is verified.

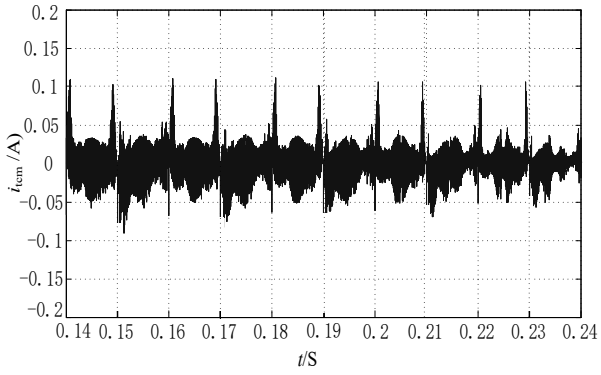

Figure 8. Simulation waveform of common-mode leakage current i_{tcm}

From the above simulation analysis, it can be seen that within the power frequency cycle, the common-mode voltage V_{NG} of the four operating modes (including shoot-through and non-shoot-through states) of the low-leakage-current quasi-Z-source photovoltaic inverter for new energy mountain agricultural machinery is the same, containing only DC and low-frequency components, with no high-frequency components. Therefore, the high-frequency common-mode leakage current of the proposed inverter can be effectively suppressed.

5. Conclusion

This paper proposes a low-leakage-current quasi-Z-source photovoltaic inverter for new energy mountain agricultural machinery, and conducts theoretical analysis and simulation verification on its topological structure, modulation strategy, and common-mode leakage current suppression mechanism. Through the above research and analysis, the following conclusions can be drawn:

(1) Compared with the bridge-type grid-connected inverter, the low-leakage-current quasi-Z-source photovoltaic inverter for new energy mountain agricultural machinery eliminates the need for dead-time, and the grid-connected current has no low-frequency harmonic components, thus achieving higher power quality.

(2) Compared with the dual-buck grid-connected inverter, by reasonably inserting shoot-through vectors into the quasi-Z-source photovoltaic grid-connected inverter, the quasi-Z-source network can effectively boost the DC bus voltage, thus effectively improving the DC voltage utilization rate of the inverter.

(3) The novel USPWM modulation strategy enables the switches to operate in a half-cycle mode, reducing switching losses. Moreover, the AC-side current in the freewheeling loop does not pass through the poor-performance body diode of the switches. Therefore, the quasi-Z-source photovoltaic grid-connected inverter not only eliminates the need for dead-time but also achieves high efficiency and reliability, low cost, and high power density.

(4) The low-leakage-current quasi-Z-source photovoltaic inverter for new energy mountain agricultural machinery has the same common-mode voltage within the power frequency cycle, and the common-mode voltage contains only DC and low-frequency components. Therefore, the quasi-Z-source photovoltaic grid-connected inverter can effectively suppress high-frequency common-mode leakage current.

Acknowledgments

This work was supported by the Yibin Municipal Science and Technology Bureau Project "Topology and Leakage Current Suppression Technology of Multi-Degree-of-Freedom Adjustable Z-Source Crystalline Silicon Photovoltaic Grid-Connected Inverter" (2024MZ003); the 2026 Central Government Guided Local Science and Technology Development Fund Project "Construction of Bijie New Comprehensive Energy Science and Technology Innovation Research Institute and Key Technology Research on Intelligent Coal Mining and Disaster Prevention and Control" (QKHZYD(2026)026); the Bijie Vocational and Technical College Research Project (XS22ZRYB-04); and the Sichuan Postdoctoral Research Project Special Funding Program (TB2023025).

References

[1] Xiao, H. F., Wang, X. B., Zhang, X., et al. (2020). State-of-the-art and future trend of transformerless photovoltaic grid-

connected inverters. *Proceedings of the CSEE*, 40(4), 1038–1054, 1397.

[2] Xiao, H. F., Xie, S. J., Chen, W. M., et al. (2010). Study on leakage current model for transformerless photovoltaic grid-connected inverter. *Proceedings of the CSEE*, 30(18), 9–14.

[3] Wu, W. Y., & Guo, X. Q. (2012). A review of novel leakage current suppression techniques for transformerless photovoltaic inverters. *Proceedings of the CSEE*, 32(18), 1–8, 170.

[4] Guo, X. Q., & Jia, X. Y. (2018). Analysis of common mode leakage current for transformerless cascaded H5 PV inverter. *Transactions of China Electrotechnical Society*, 33(2), 361–369.

[5] Wang, B. C., Guo, X. Q., Yang, Y., et al. (2018). Common mode behavior for Z-source four-leg inverter. *Transactions of China Electrotechnical Society*, 33(24), 5848–5855.

[6] Li, Y., & Peng, F. Z. (2011). Constant capacitor voltage control strategy for Z-source/quasi-Z-source inverter in grid-connected photovoltaic systems. *Transactions of China Electrotechnical Society*, 26(5), 62–69.

[7] Qu, A. W., Chen, D. L., & Su, Q. (2017). Novel single-stage three-phase voltage-fed quasi-z-source photovoltaic grid-connected inverter. *Proceedings of the CSEE*, 37(7), 2091–2101.

[8] Chen, Y., Huang, K., & Cao, Z. H. (2023). Third harmonic compensation strategy of quasi-Z-source cascaded multilevel photovoltaic grid-connected inverter. *Power System Protection and Control*, 51(9), 147–155.

[9] Zhang, Z. B., Zhang, X., Cao, R. X., et al. (2012). A new family of buck-boost grid-connected inverters. *Proceedings of the CSEE*, 32(27), 8–15, 185.

[10] Liu, F., Duan, S. X., Liu, B. Y., et al. (2007). A variable step size INC MPPT method for PV systems. *Proceedings of the CSEE*, 27(12), 50–55.

[11] Wang, B. C., Guo, X. Q., Yang, Y., et al. (2019). Common-mode voltage suppression strategy for Z-source four-leg inverter. *Transactions of China Electrotechnical Society*, 34(6), 1241–1249.

[12] Cheng, Q. M., Jiang, C., Shen, L., et al. (2020). Passivity-based control strategy of quasi Z-source three-level grid-connected inverter. *Transactions of China Electrotechnical Society*, 35(20), 4361–4372.